Journal of Mathematical Chemistry Vol. 36, No. 3, July 2004 (© 2004)

Doubly-colored graphs as graphical models for subductions of coset representations, double cosets, and unit subduced cycle indices

Shinsaku Fujita*

Department of Chemistry and Materials Technology, Kyoto Institute of Technology, Matsugasaki, Sakyo-ku, Kyoto 606-8585, Japan
E-mail: fajitas@chem.kit.ac.jp

Sherif El-Basil

Faculty of Pharmacy, Kasr El-Aini Street, Cairo 11562, Egypt

Received 8 April 2004; revised 29 June 2004

The concept of doubly-colored graphs is proposed to model subductions of coset representations, double cosets, and unit subduced cycle indices, which have been mathematically formulated in coset algebraic theory developed by Fujita (Symmetry and Combinatorial Enumeration in Chemistry, Springer-Verlag, Berlin, 1991).

KEY WORDS: coset representation, subduction, double coset, graphical model

1. Introduction

The USCI (unit-subduced-cycle-index) approach developed by Fujita [1] is based on the subduction of coset representations (CRs) [1,2]. Although this approach is versatile in combinatorial enumeration, the concept of "subduction of CRs" is not so easy to understand, because it has been originally given by purely mathematical and abstract formulation [2].

To show how mathematically it is formulated, the subduction of a coset representation is introduced briefly. A group $\mathbf{G}$ is expressed as a set of elements:

$$\mathbf{G} = \left\{g_1, g_2, \ldots, g_{|\mathbf{G}|}\right\}, \tag{1}$$

where $|\mathbf{G}|$ is the order of $\mathbf{G}$ and $g_1 = I$ (the identity element). The set of elements generates a sequence of subgroups (SSG), which are usually ordered in a non-descending way of their orders:

$$\mathrm{SSG} = \{\mathbf{G}_1, \mathbf{G}_2, \ldots, \mathbf{G}_s\}, \tag{2}$$

* Corresponding author.

0259-9791/04/0700-0211/0

where each subgroup is a representative of relevant conjugate subgroups within $\mathbf{G}$ and we place $\mathbf{G}_1 = \mathbf{C}_1 = \{I\}$ and $\mathbf{G}_s = \mathbf{G}$. Each subgroup $\mathbf{G}_i$ ($1 \leqslant i \leqslant s$) selected as a representative of conjugate subgroups may be used to express $\mathbf{G}$ as a (right) coset so as to give a coset decomposition expressed by

$$\mathbf{G} = \mathbf{G}_i g_1 + \mathbf{G}_i g_2 + \cdots + \mathbf{G}_i g_r. \tag{3}$$

As a result, we obtain a set of cosets defined by

$$\mathbf{G}/\mathbf{G}_i = \{\mathbf{G}_i g_1, \mathbf{G}_i g_2, \ldots, \mathbf{G}_i g_r\}, \tag{4}$$

where r represents the number of cosets in the coset decomposition (equation (3)). By multiplying each coset by g ($\in \mathbf{G}$), equation (4) generates a permutation π_g as follows:

$$\pi_g = \begin{pmatrix} \mathbf{G}_i g_1 & \mathbf{G}_i g_2 & \cdots & \mathbf{G}_i g_r \\ \mathbf{G}_i g_1 g & \mathbf{G}_i g_2 g & \cdots & \mathbf{G}_i g_r g \end{pmatrix}. \tag{5}$$

When g runs over $\mathbf{G}$, we obtain a set of permutations $\mathbf{G}(/\mathbf{G}_i)$ given by

$$\mathbf{G}(/\mathbf{G}_i) = \{\pi_g \mid \forall g \in \mathbf{G}\}. \tag{6}$$

The set of permutations (equation (6)) is called *coset representation*, the symbol of which has been coined as $\mathbf{G}(/\mathbf{G}_i)$ in order to emphasize the distinction between the global ($\mathbf{G}$) and the local symmetry ($\mathbf{G}_i$) [3]. When we select π_g for g ($\in \mathbf{G}_j$), we obtain a restricted set represented by

$$\mathbf{G}(/\mathbf{G}_i) \downarrow \mathbf{G}_j = \{\pi_g \mid \forall g \in \mathbf{G}_j\} \tag{7}$$

which is called *subduction of the coset representation*. During this process, the transitivity of $\mathbf{G}(/\mathbf{G}_i)$ (equation (6)) is influenced so as to generate one or more orbits, which are in turn controlled by coset representations of $\mathbf{G}_j$. Fujita showed how to calculate the subduction pattern generated during the process of the restriction by $\mathbf{G}_j$ by using a table of marks [1,2]. Thereby, he formulated the subduction pattern as follows:

$$\mathbf{G}(/\mathbf{G}_i) \downarrow \mathbf{G}_j = \beta_{jk}\mathbf{G}_j(/\mathbf{G}_k) + \beta_{j\ell}\mathbf{G}_j(/\mathbf{G}_\ell) + \cdots, \tag{8}$$

where $\mathbf{G}_i$, $\mathbf{G}_j$, $\mathbf{G}_k$, and $\mathbf{G}_\ell$ are all subgroups of $\mathbf{G}$, while $\mathbf{G}_k$, $\mathbf{G}_\ell$, ... are subgroups of the (subducing) subgroup $\mathbf{G}_j$. According to equation (8), monomial expressions called *unit subduced cycle indices* (USCIs) are obtained as general formulas [1,2]:

$$s_{d_{jk}}^{\beta_{jk}} s_{d_{j\ell}}^{\beta_{j\ell}} \cdots, \tag{9}$$

where we place $d_{jk} = |\mathbf{G}_j|/|\mathbf{G}_k|$, $d_{j\ell} = |\mathbf{G}_j|/|\mathbf{G}_\ell|$, and so on and select the superscripts from the multiplicity factors β_{jk}, β_{jk}, etc. in equation (8). Naturally, when $\mathbf{G}_i$ is equal to $\mathbf{C}_1 = \{I\}$ in equation (6), the regular representation $\mathbf{G}(/\mathbf{C}_1)$ results.

For the purpose of applying such CRs and their subductions to combinatorial enumeration, we should take account of two aspects. First, CRs and their subduction control orbits (equivalence classes) of ligands or vertices in a molecule or graph [4–6]. Second, they also control orbits (equivalence classes) of isomeric molecules or graphs (configurations) [1,2]. Understanding the relationship between the two aspects is essential to gain a deeper insight to combinatorial enumeration (cf. chapter 15 of [1]). Although a few graphical studies have recently appeared with respect to the two aspects of CRs [7,8], there have been no graphical studies on the two aspects for the concept of subduction to the best of our knowledge. In fact, one recent study for modeling subduction of CRs has stressed the latter aspect, where it has used Cayley graphs in its formulation [9]. Hence, it is desirable to develop a graphical or non-mathematical approach which is capable of giving a balanced perspective on the two aspects. Moreover, because the Cayley graphs are still a rather mathematical tool which is not familiar to experimental chemists, a more direct way of modeling would be desirable to clarify both the two aspects underlying the concepts of subduction of CRs and USCIs. In summary, it is the main objective of this work to model the concepts of subduction of CRs and USCIs by developing *double coloring* of graphs as a new concept, which can provide experimental chemists with a concrete image of the abstract concepts. In addition, the double coloring is applied to the modeling of double cosets.

2. Regular bodies as parent graphs

To model CRs of a group $\mathbf{G}$, we start from a regular body as a parent graph, which contains $|\mathbf{G}|$ equivalent vertices (substituted by an appropriate ligand, i.e., $\circ$) [4]. The set of $|\mathbf{G}|$ positions construct an orbit (equivalence class), which is controlled by the regular representation $\mathbf{G}(/\mathbf{C}_1)$ of degree $|\mathbf{G}|$. Since the regular body itself stays fixed under the action of all of the elements of $\mathbf{G}$, it can be considered to be a single uncolored graph as a homomer. In other words, the homomer set contains only one homomer, which is represented by the symbol, $\mathcal{H}[\mathbf{G}(/\mathbf{G})] = \{h\}$.

Figure 1 illustrates several regular bodies which we use as parent graphs in this paper. As a parent graph of $\mathbf{D}_{2d}$-symmetry, we use an allene derivative (**1**), the derivation of which has been discussed previously [6]. For the sake of convenience, we adopt a top view (**2**) through the C_2-axis. As a parent graph of $\mathbf{C}_{2v}$-symmetry, we use a cyclopropane segment (**3**) selected from the allene derivative (**1**). We adopt a top view (**4**) also for this parent graph. To differentiate between parent graphs of $\mathbf{C}_s$- and $\mathbf{C}_2$-symmetry, we adopt **5** and **6** with perpendicular arrow symbols.

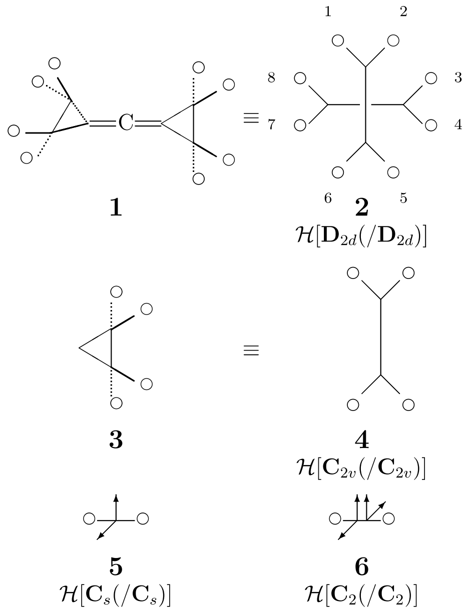

Figure 1. Several regular bodies as parent graphs.

3. Homomer sets controlled by CRs

According to lemma 7.1 of [1] and lemma 2 of [4], we can select sets of $|\mathbf{G}_i|$ vertices from the $|\mathbf{G}|$, where each of the selected sets belongs to the $\mathbf{G}_i$-symmetry. The number of such sets is equal to $|\mathbf{G}|/|\mathbf{G}_i|$, which is given by equation (7.3) of [1]:

$$\mathbf{G}(/\mathbf{C}_1) \downarrow \mathbf{G}_i = \frac{|\mathbf{G}|}{|\mathbf{G}_i|}\mathbf{G}_i(/\mathbf{C}_1). \tag{10}$$

This equation indicates that the vertices of such an appropriate set are colored in black so as to give a colored graph of $\mathbf{G}_i$. This derivation has once been discussed in detail in terms of subductive and inductive derivation [6]. The resulting colored graph, h_1, is operated upon by the elements of $\mathbf{G}$ to generate the full set of (symmetry equivalent) graphs, which is called *homomer set* represented by the symbol $\mathcal{H}[\mathbf{G}(/\mathbf{G}_i)] = \{h_1, h_2, \ldots, h_r\}$, where $r = |\mathbf{G}|/|\mathbf{G}_i|$. In place of the use of all the elements, we can use the representatives of the cosets, i.e., $\{g_1, g_2, \ldots, g_r\}$, which appear in equation (4). The homomers in $\mathcal{H}[\mathbf{G}(/\mathbf{G}_i)]$ are controlled by the coset representation $\mathbf{G}(/\mathbf{G}_i)$ (equation (6)), because they correspond to the cosets represented by equation (4). This has been generally proved previously (theorem 15.2 of [1]). It should be noted that the present term "homomer" designates both homomers and enantiomers from the stereochemical point of view.

Let us consider an allene skeleton of the $\mathbf{D}_{2d}$-symmetry (**2**) as a parent graph. The $\mathbf{D}_{2d}$-group contains the following elements:

$$\mathbf{D}_{2d} = \{I, C_{2(3)}, C_{2(1)}, C_{2(2)}, \sigma_{d(1)}, \sigma_{d(2)}, S_4, S_4^3\}, \tag{11}$$

where the element $C_{2(3)}$ is selected as the two-fold axis along with the C=C=C axis of allene.

Let us examine $\mathbf{G}_i = \mathbf{C}_s = \{I, \sigma_{d(1)}\}$, which is one of the eight subgroups of $\mathbf{D}_{2d}$ (up to conjugacy). Then, the cosets of this case are obtained as follows according to equation (4):

$$\begin{aligned} 1 &: \mathbf{C}_s = \mathbf{C}_s I = \{I, \sigma_{d(1)}\}, \\ 2 &: \mathbf{C}_s C_{2(3)} \quad = \{C_{2(3)}, \sigma_{d(2)}\}, \\ 3 &: \mathbf{C}_s C_{2(1)} \quad = \{C_{2(1)}, S_4\}, \\ 4 &: \mathbf{C}_s C_{2(2)} \quad = \{C_{2(2)}, S_4^3\} \end{aligned} \tag{12}$$

from which we select the representatives to give the following transversal:

$$T_{\mathbf{D}_{2d}/\mathbf{C}_1} = \{I, C_{2(3)}, C_{2(1)}, C_{2(2)}\}. \tag{13}$$

According to equation (10), we have the following equation:

$$\mathbf{D}_{2d}(/\mathbf{C}_1) \downarrow \mathbf{C}_s = \frac{|\mathbf{D}_{2d}|}{|\mathbf{C}_s|}\mathbf{C}_s(/\mathbf{C}_1) = 4\mathbf{C}_s(/\mathbf{C}_1), \tag{14}$$

which produces a partition of vertices (1 2)(3 8)(4 7)(5 6) in **2** shown in figure 1. By coloring the first set of vertices (1 2) in black, we obtain the graph **7** (h_1 shown in figure 2), which belongs to the $\mathbf{C}_s$-symmetry according to equation (14).

By applying the element $\sigma_{d(1)}$ of $\mathbf{C}_2 I$ (= $\mathbf{C}_s$) to the first graph **7** (h_1), we can obtain the identical graph (**7**′), although the numbering of the vertices is altered. Thus, coset 1 ($\mathbf{C}_2 I$) shown in equation (12) corresponds to the set of **7** and **7**′, which is represented by h_1 as a generator graph. According to the cosets listed in equation (12), the elements of coset 2 ($\mathbf{C}_s C_{2(3)}$) generate the set of **8** and **8**′, which is a homomer represented by h_2; the elements of coset 3 ($\mathbf{C}_s C_{2(1)}$) generate the set of **9** and **9**′ (h_3); and the elements of coset 4 ($\mathbf{C}_s C_{2(2)}$) generate the set of **10** and **10**′ (h_4). Thereby, we can obtain a homomer set $\mathcal{H}[\mathbf{D}_{2d}(/\mathbf{C}_s)]$ by collecting the four homomers to give $\mathcal{H}[\mathbf{D}_{2d}(/\mathbf{C}_s)] = \{h_1, h_2, h_3, h_4\}$. Note that the homomer set can also be obtained by operating the transversal (equation (13)) on h_1. It follows that the set $\mathcal{H}[\mathbf{D}_{2d}(/\mathbf{C}_s)]$ exhibits the one-to-one correspondence represented by $h_1 \to 1$, $h_2 \to 2$, $h_3 \to 3$, and $h_4 \to 4$, where the cosets at issue are numbered as shown in equation (12). As a result, the set $\mathcal{H}[\mathbf{D}_{2d}(/\mathbf{C}_s)]$ is controlled by the coset representation $\mathbf{D}_{2d}(/\mathbf{C}_s)$.

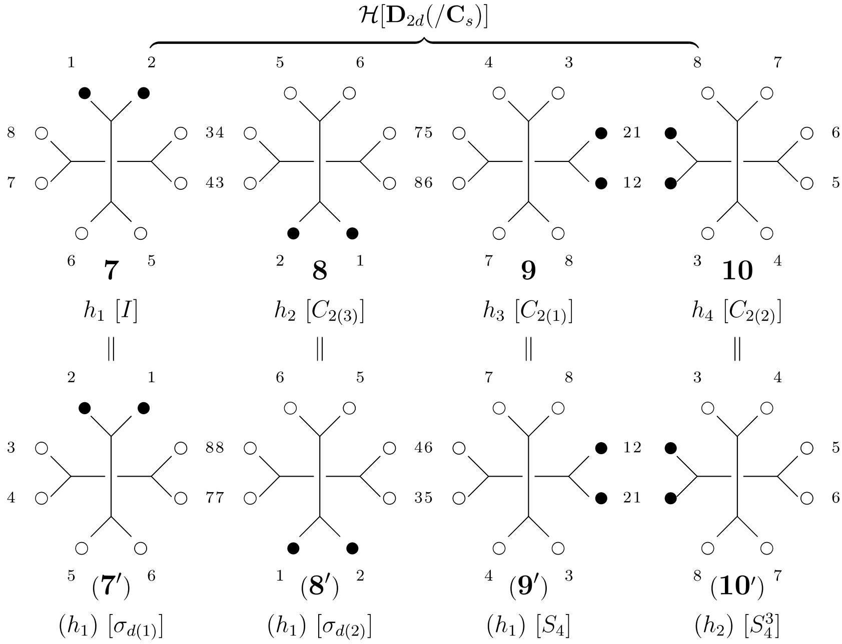

Figure 2. Four homomers which model $\mathbf{D}_{2d}(/\mathbf{C}_s)$, i.e., $\mathcal{H}[\mathbf{D}_{2d}(/\mathbf{C}_s)] = \{h_1, h_2, h_3, h_4\}$.

Let us next examine $\mathbf{G}_i = \mathbf{C}_2 = \{I, C_{2(3)}\}$, which is one of the eight subgroups of $\mathbf{D}_{2d}$ (up to conjugacy). Then, the cosets of this case are obtained as follows according to equation (4):

$$\begin{aligned} 1 &: \mathbf{C}_2 = \mathbf{C}_2 I = \{I, C_{2(3)}\}, \\ 2 &: \mathbf{C}_2\sigma_{d(1)} \quad = \{\sigma_{d(1)}, \sigma_{d(2)}\}, \\ 3 &: \mathbf{C}_2 S_4 \qquad = \{S_4, S_4^3\}, \\ 4 &: \mathbf{C}_2 C_{2(1)} \quad = \{C_{2(1)}, C_{2(2)}\}. \end{aligned} \tag{15}$$

According to equation (10), we have the following equation:

$$\mathbf{D}_{2d}(/\mathbf{C}_1) \downarrow \mathbf{C}_2 = \frac{|\mathbf{D}_{2d}|}{|\mathbf{C}_2|}\mathbf{C}_2(/\mathbf{C}_1) = 4\mathbf{C}_2(/\mathbf{C}_1), \tag{16}$$

which produces a partition of vertices (1 5)(2 6)(3 7)(4 8) in the regular body (**2**) shown in figure 1. Hence, by coloring the two vertices (1 5) in black, we can obtain a colored graph h_1 of $\mathbf{C}_2$-symmetry, as shown in figure 3. By applying the representative $\sigma_{d(1)}$ of the coset $\mathbf{C}_2\sigma_{d(1)}$ (equation (15)) to the first homomer h_1, we can obtain the second homomer h_2. On the same line, the applications of S_4 ($\in \mathbf{C}_2 S_4$) and $C_{2(1)}$ ($\in \mathbf{C}_2 C_{2(1)}$) yield homomers h_3 and h_4, respectively. As a result, it can be shown that the set $\mathcal{H}[\mathbf{D}_{2d}(/\mathbf{C}_2)]$ exhibits the one-to-one correspondence represented by $h_1 \to 1$, $h_2 \to 2$, $h_3 \to 3$, and $h_4 \to 4$, where the cosets at issue are numbered as shown in equation (15). As a result, the set $\mathcal{H}[\mathbf{D}_{2d}(/\mathbf{C}_2)]$

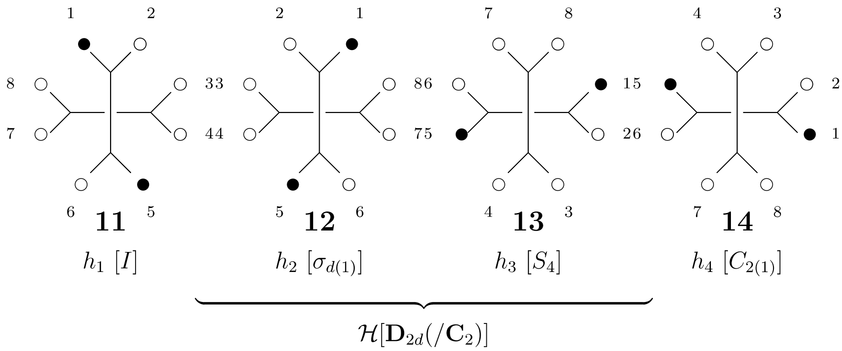

Figure 3. Four homomers which model $\mathbf{D}_{2d}(/\mathbf{C}_2)$, i.e., $\mathcal{H}[\mathbf{D}_{2d}(/\mathbf{C}_2)] = \{h_1, h_2, h_3, h_4\}$.

is controlled by the coset representation $\mathbf{D}_{2d}(/\mathbf{C}_2)$. Strictly speaking, the pair of h_1 and h_2 or the pair of h_3 and h_4 exhibits an enantiomeric pair from the stereochemical point of view. For the sake of simplicity, however, the four graphs of the two pairs are referred to as homomers in this paper.

4. Double coloring for modeling of subductions of CRs

4.1. Doubly-colored graphs

4.1.1. Doubly-colored parent graphs

To discuss a direct model of $\mathbf{G}(/\mathbf{G}_i) \downarrow \mathbf{G}_j$, we first consider a special case of $\mathbf{G}(/\mathbf{G}) \downarrow \mathbf{G}_j$. The corresponding homomer set $\mathcal{H}[\mathbf{G}(/\mathbf{G})]$ contains only one (uncolored) graph (the parent graph). Since we can easily find the following subduction as a rather trivial case:

$$\mathbf{G}(/\mathbf{G}) \downarrow \mathbf{G}_j = \mathbf{G}_j(/\mathbf{G}_j), \tag{17}$$

we obtain a homomer set $\mathcal{H}[\mathbf{G}_j(/\mathbf{G}_j)]$ which contains one (uncolored) graph. This rather trivial case corresponds to the double coloring of vertices, which is a kind of coloring (additive coloring by large circle/none) other than the vertex coloring (single coloring by black/white) described in the preceding paragraphs.

For example, the graph **15** shown in figure 4 illustrates a direct model for the subduction $\mathbf{D}_{2d}(/\mathbf{D}_{2d}) \downarrow \mathbf{C}_{2v} = \mathbf{C}_{2v}(/\mathbf{C}_{2v})$, where the vertices 1, 2, 5, and 6 of **2** are colored by (substituted) by large circles superimposed onto small open circles. Thereby, the resulting graph (**15**) belongs to $\mathbf{C}_{2v}$-symmetry, where the set of the equivalent vertices 1, 2, 5, and 6 is differentiated from the set of vertices 3, 4, 7, and 8. We call this type of colored graph *doubly-colored graphs* for the sake of convenience. The two sets of vertices are controlled by the subduction represented by

$$\mathbf{D}_{2d}(/\mathbf{C}_1) \downarrow \mathbf{C}_{2v} = 2\mathbf{C}_{2v}(/\mathbf{C}_1), \tag{18}$$

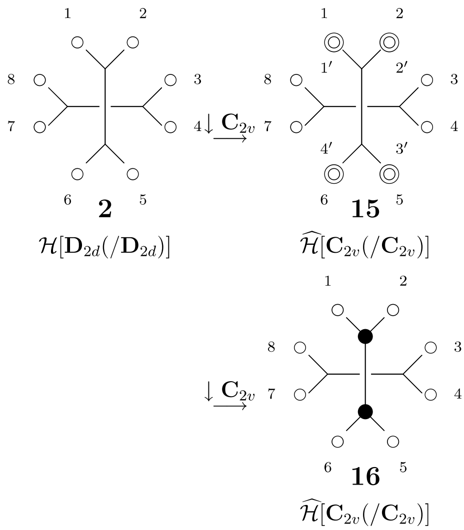

Figure 4. Direct modeling of a group subduction represented by $\mathbf{D}_{2d}(/\mathbf{D}_{2d}) \downarrow \mathbf{C}_{2v} = \mathbf{C}_{2v}(/\mathbf{C}_{2v})$.

which is a concrete case of equation (10). Each of the two sets corresponds to a homomer set $\widehat{\mathcal{H}}[\mathbf{C}_{2v}(/\mathbf{C}_{2v})]$, where the symbol with a hat is used to designated such a homomer as containing doubly-colored graphs. Its correspondence to the parent graph **4** for $\mathcal{H}[\mathbf{C}_{2v}(/\mathbf{C}_{2v})]$ shown in figure 1 can be easily understood by inspection.

If chemical meanings are required, the double coloring can be considered to be the introduction of the corresponding isotopes. Thus, let the symbols ○ and ● represent a hydrogen atom and a chlorine atom. Then, their double colored forms ◎ and ◉ represent a deuterium atom (^{2}H) and ^{37}Cl respectively.

If other chemical meanings are required, we can consider the graph **16** for modeling $\mathbf{D}_{2d}(/\mathbf{D}_{2d}) \downarrow \mathbf{C}_{2v} = \mathbf{C}_{2v}(/\mathbf{C}_{2v})$, where both of the two carbons of a cyclopropane are substituted (colored) by solid circles (●, e.g., ^{13}C) to restrict the symmetry of the parent graph into $\mathbf{C}_{2v}$. Thereby, the set of vertices 1, 2, 5, and 6 in **16** is differentiated from the set of vertices 3, 4, 7, and 8. During this process, the four equivalent carbons in **2**, which are governed by $\mathbf{D}_{2d}(/\mathbf{C}_s)$, are divided into two sets according to the following subduction:

$$\mathbf{D}_{2d}(/\mathbf{C}_s) \downarrow \mathbf{C}_{2v} = \mathbf{C}_{2v}(/\mathbf{C}_s) + \mathbf{C}_{2v}(/\mathbf{C}'_s), \tag{19}$$

which has once been discussed in detail in chapter 9 of [1].

4.1.2. *Vertices of Doubly-Colored Parent Graphs*

Let us consider a regular body as a parent graph for modeling the group $\mathbf{G}$, where its $|\mathbf{G}|$ vertices correspond to the elements of $\mathbf{G}$. This means that, when $\mathbf{G}$ is regarded as an ordered set, the vertices of the regular body can be numbered sequentially according to the order of (1), i.e., $1, 2, \ldots, |\mathbf{G}|$. This nature is characterized by the statement that the vertices of the regular body are governed by the coset representation $\mathbf{G}(/\mathbf{C}_1)$ (the regular representation in this case). Such modes of numbering are presented in $|\mathbf{G}|!$ ways, where any one of them can be selected as a reference or a starting mode of numbering. This correspondence has been generally discussed in detail in a previous paper [5].

Let us next consider the cosets of the group $\mathbf{G}_j$:

$$\mathbf{G}/\mathbf{G}_j = \left\{\mathbf{G}_j g'_1, \mathbf{G}_j g'_2, \ldots, \mathbf{G}_j g'_{|\mathbf{G}|/|\mathbf{G}_j|}\right\}. \tag{20}$$

Each coset $\mathbf{G}_j g$ ($g \in \{g'_1, g'_1, \ldots, g'_{|\mathbf{G}|/|\mathbf{G}_j|}\}$) appearing in equation (20) can be regarded as an ordered set in which the order of its elements is the same as that of the elements of the group $\mathbf{G}_j$:

$$\begin{aligned} \mathbf{G}_j &= \{g_1^{(j)}, g_2^{(j)}, \ldots, g_{|\mathbf{G}_j|}^{(j)}\}, \\ \mathbf{G}_j g &= \{g_1^{(j)} g, g_2^{(j)} g, \ldots, g_{|\mathbf{G}_j|}^{(j)} g\}. \end{aligned} \tag{21}$$

This means that the elements of each coset can be numbered sequentially according to the order of equation (21), i.e., $1', 2', \ldots, |\mathbf{G}_j|'$. Such modes of numbering are presented in $|\mathbf{G}_j|!$ ways, where any one of them can be selected as a reference or a starting mode of numbering. Note that the numbering based on equation (21) can be selected in this way to correspond to the one based on equation (1).

Keeping this correspondence (equation (21)) in mind, all of the elements of $\mathbf{G}$ are operated on the numbered regular body as a starting graph. When $g\,(\in \mathbf{G}_j g)$ is operated on the numbered regular body, we adopt the changed numbering based on the changed order of equation (1) as well as the changed numbering based on the changed order of equation (21). The former numbering corresponds to $\mathbf{G}(/\mathbf{G})$ (and $\mathbf{G}(/\mathbf{C}_1)$ for its vertices) and the latter numbering corresponds to $\mathbf{G}_j(/\mathbf{G}_j)$ (and $\mathbf{G}_j(/\mathbf{C}_1)$ for its vertices), as shown in equation (17).

For example, the vertices of the regular body **2** of $\mathbf{D}_{2d}$ can be numbered according to the order:

$$\begin{array}{cccccccc} \{I & \sigma_{d(1)} & S_4 & C_{2(1)} & C_{2(3)} & \sigma_{d(2)} & S_4^3 & C_{2(2)}\} \\ 1 & 2 & 3 & 4 & 5 & 6 & 7 & 8 \end{array} \tag{22}$$

to give the numbering shown in figure 4.

According to the coset decomposition $\mathbf{D}_{2d} = \mathbf{C}_{2v} + \mathbf{C}_{2v} S_4$, we obtain the numbering shown in **15**:

$$\begin{array}{cccc|cccc} \{I & \sigma_{d(1)} & C_{2(3)} & \sigma_{d(2)} & S_4 & C_{2(1)} & S_4^3 & C_{2(2)}\} \\ 1 & 2 & 5 & 6 & 3 & 4 & 7 & 8 \\ 1' & 2' & 3' & 4' & 1' & 2' & 3' & 4' \end{array}\ . \tag{23}$$

We select **15** as a starting graph, which is permutated on the action of all of the elements of $\mathbf{D}_{2d}$. The resulting eight modes of numbering are listed in figure 5, where we adopt the numbering according to equation (22) and the numbering according to equation (23). The resulting set of **15**, **17**, **20**, and **21**, which are identical to each other, indicates a graph of $\mathbf{C}_{2v}$-symmetry. The set is characterized by the CR, $\mathbf{C}_{2v}(/\mathbf{C}_{2v})$. The other set of **18**, **19**, **22**, and **23** are identical to give a graph of $\mathbf{C}_{2v}$-symmetry. The set is also characterized by the CR, $\mathbf{C}_{2v}(/\mathbf{C}_{2v})$.

Note that the former set (**15**, **17**, **20**, and **21**) is based on the numbering according to the coset $\mathbf{C}_{2v}I$ (equation (23)), while the latter set (**18**, **19**, **22**, and **23**) is based on the numbering according to the coset $\mathbf{C}_{2v}S_4$ (equation (23)).

By the inspection of figure 5, we can understand that the subduction by $\mathbf{C}_{2v}$ (i.e., $\mathbf{D}_{2d}(/\mathbf{D}_{2d}) \downarrow \mathbf{C}_{2v}$ for a parent graph and $\mathbf{D}_{2d}(/\mathbf{C}_1) \downarrow \mathbf{C}_{2v}$ for its vertices) is regarded as the restriction of numbering from $\mathbf{D}_{2d}$ to $\mathbf{C}_{2v}$ in terms of the corresponding cosets of $\mathbf{D}_{2d}/\mathbf{C}_{2v}$ as ordered sets. Obviously, this holds true for general cases.

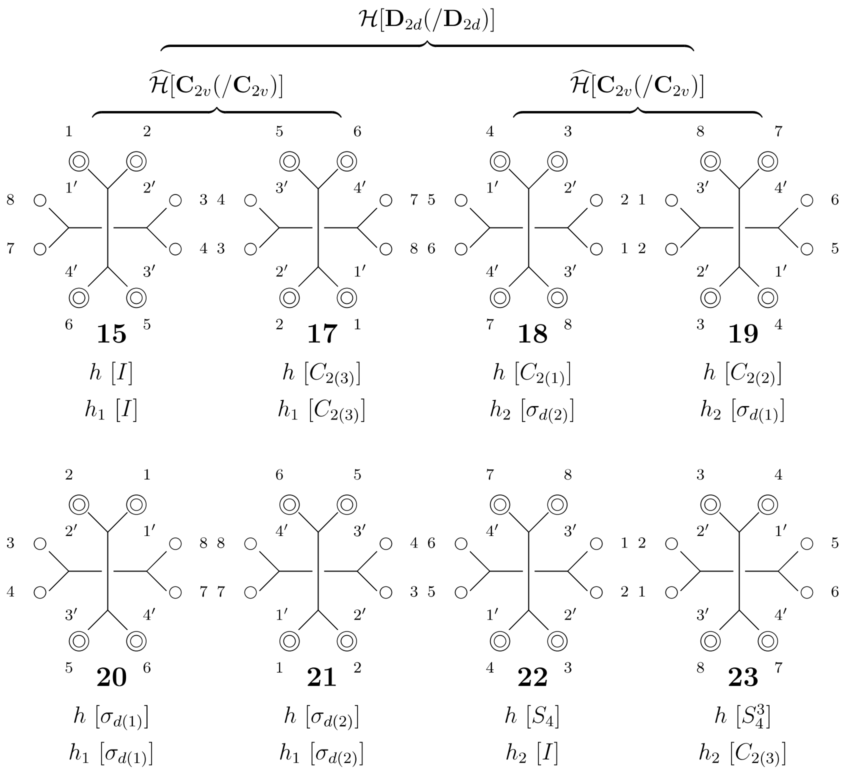

Figure 5. Eight graphs for modeling $\mathbf{D}_{2d}(/\mathbf{D}_{2d})$ and two sets of four graphs for modeling $\mathbf{C}_{2v}(/\mathbf{C}_{2v})$. This means that $\mathcal{H}[\mathbf{D}_{2d}(/\mathbf{D}_{2d})] = \{h\}$ and $\widehat{\mathcal{H}}[\mathbf{C}_{2v}(/\mathbf{C}_{2v})] = \{h_1\}$ or $\{h_2\}$.

4.2. Double coloring of homomer sets

To model the subduction $\mathbf{G}(/\mathbf{G}_i) \downarrow \mathbf{G}_j$, we define *double coloring* in which we combine the homomer set $\mathcal{H}[\mathbf{G}(/\mathbf{G}_i)]$ of the vertex coloring and the homomer set of the additive coloring $\widehat{\mathcal{H}}[\mathbf{G}_j(/\mathbf{G}_j)]$. For example, we combine $\mathcal{H}[\mathbf{D}_{2d}(/\mathbf{C}_s)]$ (figure 2) with $\widehat{\mathcal{H}}[\mathbf{C}_{2v}(/\mathbf{C}_{2v})]$ (figure 5) in order to model the subduction $\mathbf{D}_{2d}(/\mathbf{D}_s) \downarrow \mathbf{C}_{2v}$, Thereby, we obtain doubly-colored graphs collected in figure 6. The set of graphs (**24** and **28**) is fixed under the action of $\mathbf{C}_s$; and the set of graphs (**25** and **29**) is fixed under the action of $\mathbf{C}_s$. This means that these two sets satisfies $\widehat{\mathcal{H}}[\mathbf{C}_{2v}(/\mathbf{C}_s)] = \{\hat{h}_1, \hat{h}_2\}$. On the other hand, the set of graphs (**26** and **30**) is fixed under the action of $\mathbf{C}'_s$; and the set of graphs (**27** and **31**) is fixed under the action of $\mathbf{C}'_s$. This means that these two sets satisfies $\widehat{\mathcal{H}}[\mathbf{C}_{2v}(/\mathbf{C}_s)] = \{\hat{h}'_1, \hat{h}'_2\}$.

The reasoning of the double coloring process for obtaining $\widehat{\mathcal{H}}[\mathbf{C}_{2v}(/\mathbf{C}_s)]$ and $\widehat{\mathcal{H}}[\mathbf{C}_{2v}(/\mathbf{C}'_s)]$ (figure 6) from $\mathcal{H}[\mathbf{D}_{2d}(/\mathbf{C}_s)]$ (figure 2) and $\widehat{\mathcal{H}}[\mathbf{C}_{2v}(/\mathbf{C}_{2v})]$ (figure 5) is complicated, as explained above. It is, however, easy to apply the double coloring

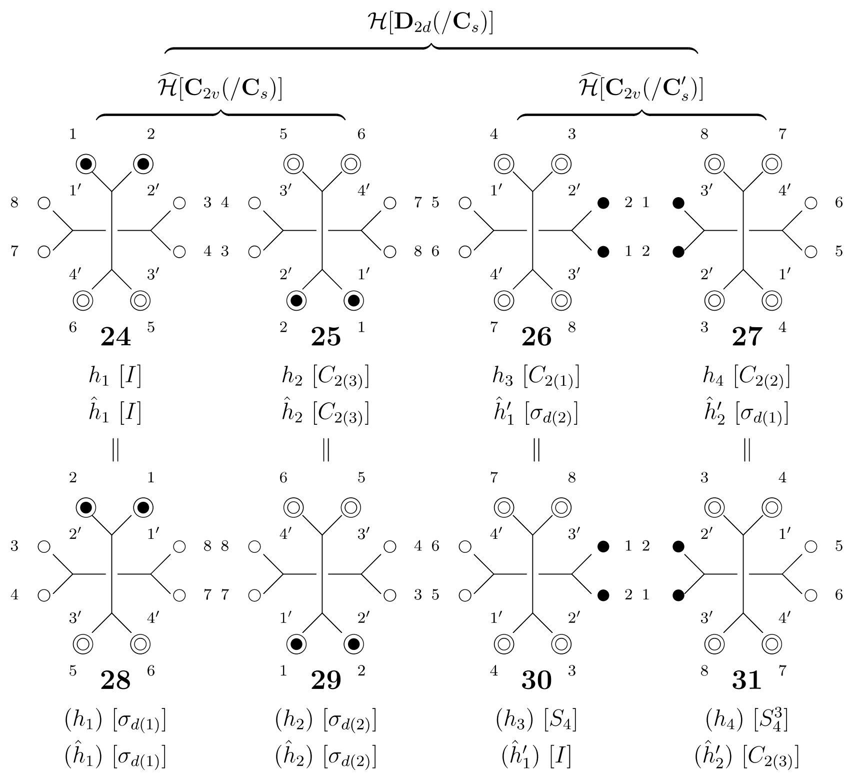

Figure 6. Double coloring for modeling $\mathbf{D}_{2d}(/\mathbf{D}_s) \downarrow \mathbf{C}_{2v}$. This means that $\mathcal{H}[\mathbf{C}_{2v}(/\mathbf{C}_s)] = \{\hat{h}_1, \hat{h}_2\}$ and $\widehat{\mathcal{H}}[\mathbf{C}_{2v}(/\mathbf{C}'_s)] = \{\hat{h}'_1, \hat{h}'_2\}$.

to actual cases, as summarized to give figure 7, where the top row of figure 2 and the top row of figure 6 are selected to give the top and middle rows of figure 7. The bottom row (the set of **32** and **33** and the set of **34** and **35**) is obtained by starting from the parent graph (**4**) for $\mathbf{C}_{2v}(/\mathbf{C}_{2v})$ in order to model $\mathbf{C}_{2v}(/\mathbf{C}_s) + \mathbf{C}_{2v}(/\mathbf{C}'_s)$. The relationship between the middle row and the bottom row is obvious by inspection.

Figure 8 shows the conceptually same process as that of figure 7 by using an alternative additive coloring based on **16** shown in figure 4. This example may be more chemical as compared with the double coloring shown in figure 7.

Let us next model the subduction $\mathbf{D}_{2d}(/\mathbf{C}_s) \downarrow \mathbf{C}_s$. The resulting doubly-colored graphs are shown in the middle row of figure 9. Each of the doubly-colored graphs **40** and **41** is contained in a respective homomer set $\widehat{\mathcal{H}}[\mathbf{C}_s(/\mathbf{C}_s)]$. The set of **42** and **43** is contained in the homomer set $\widehat{\mathcal{H}}[\mathbf{C}_s(/\mathbf{C}_1)]$, where **42** and **43** are enantiomeric. The bottom row (the one-membered set of **44**, the one-membered set of **45**, and the two-membered set of **46** and **47**) is obtained by starting from the parent graph (**5**) for $\mathbf{C}_s(/\mathbf{C}_s)$ in order to model $2\mathbf{C}_s(/\mathbf{C}_s) + \mathbf{C}_s(/\mathbf{C}_1)$. The relationship between the middle row and the bottom row is obvious by inspection.

Doubly-colored graphs for modeling the subduction $\mathbf{D}_{2d}(/\mathbf{C}_s) \downarrow \mathbf{C}_2$ are collected in the middle row of figure 10. The set of homomers (**48** and **49**) and the other set of homomers (**50** and **51**) respectively construct homomer sets representing $\widehat{\mathcal{H}}[\mathbf{C}_2(/\mathbf{C}_1)]$. The bottom row (the two-membered set of **52** and **53**, and the two-membered set of **54** and **55**) is obtained by starting from the parent graph (**6**) for $\mathbf{C}_2(/\mathbf{C}_2)$ in order to model $2\mathbf{C}_2(/\mathbf{C}_1)$. The relationship between the middle row and the bottom row is obvious by inspection.

Let us now consider the homomer set (**11**, **12**, **13**, and **14**) listed in figure 3. Doubly-colored graphs for modeling the subduction $\mathbf{D}_{2d}(/\mathbf{C}_2) \downarrow \mathbf{C}_{2v}$ are collected in the middle row of figure 11. The set of homomers (**56** and **57**) and the other set of homomers (**58** and **59**) respectively construct homomer sets representing $\widehat{\mathcal{H}}[\mathbf{C}_{2v}(/\mathbf{C}_2)]$. In the present case, each set contains enantiomers. The bottom row (the two-membered set of **60** and **61** and the two-membered set of **62** and **63**) is obtained by starting from the parent graph (**4**) for $\mathbf{C}_{2v}(/\mathbf{C}_{2v})$ in order to model $2\mathbf{C}_{2v}(/\mathbf{C}_2)$. The relationship between the middle row and the bottom row is obvious by inspection.

5. Double coloring for modeling double cosets

We have discussed the relationship between subduction of coset representations and double cosets [10]. When the group **G** is decomposed into the following double coset decomposition:

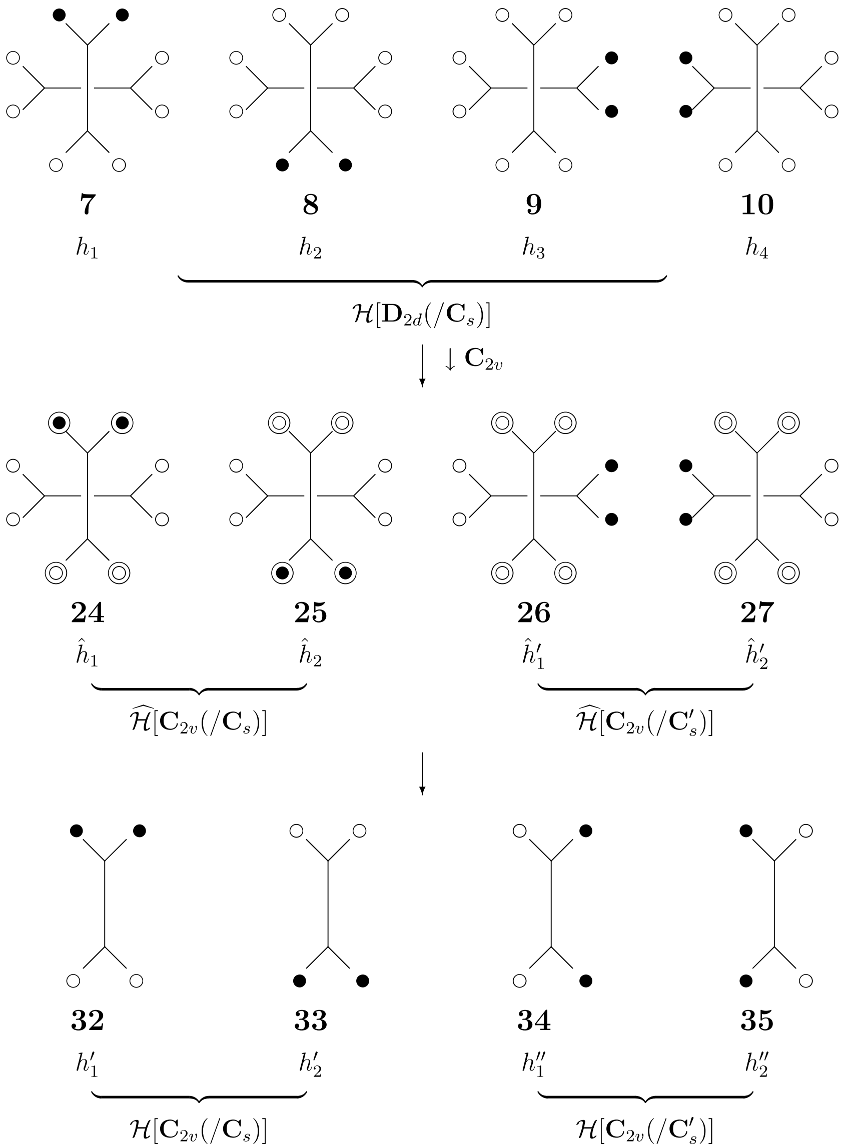

Figure 7. Double Coloring for modeling a group subduction represented by $\mathbf{D}_{2d}(/\mathbf{C}_s) \downarrow \mathbf{C}_{2v} = \mathbf{C}_{2v}(/\mathbf{C}_s) + \mathbf{C}_{2v}(/\mathbf{C}'_s)$.

$$\mathbf{G} = \mathbf{G}_i g'_1 \mathbf{G}_j + \mathbf{G}_i g'_2 \mathbf{G}_j + \cdots \mathbf{G}_i g'_{r'} \mathbf{G}_j, \tag{24}$$

where the transversal is placed as follows:

$$\Upsilon = \{g'_1, g'_2, \ldots, g'_{r'}\}. \tag{25}$$

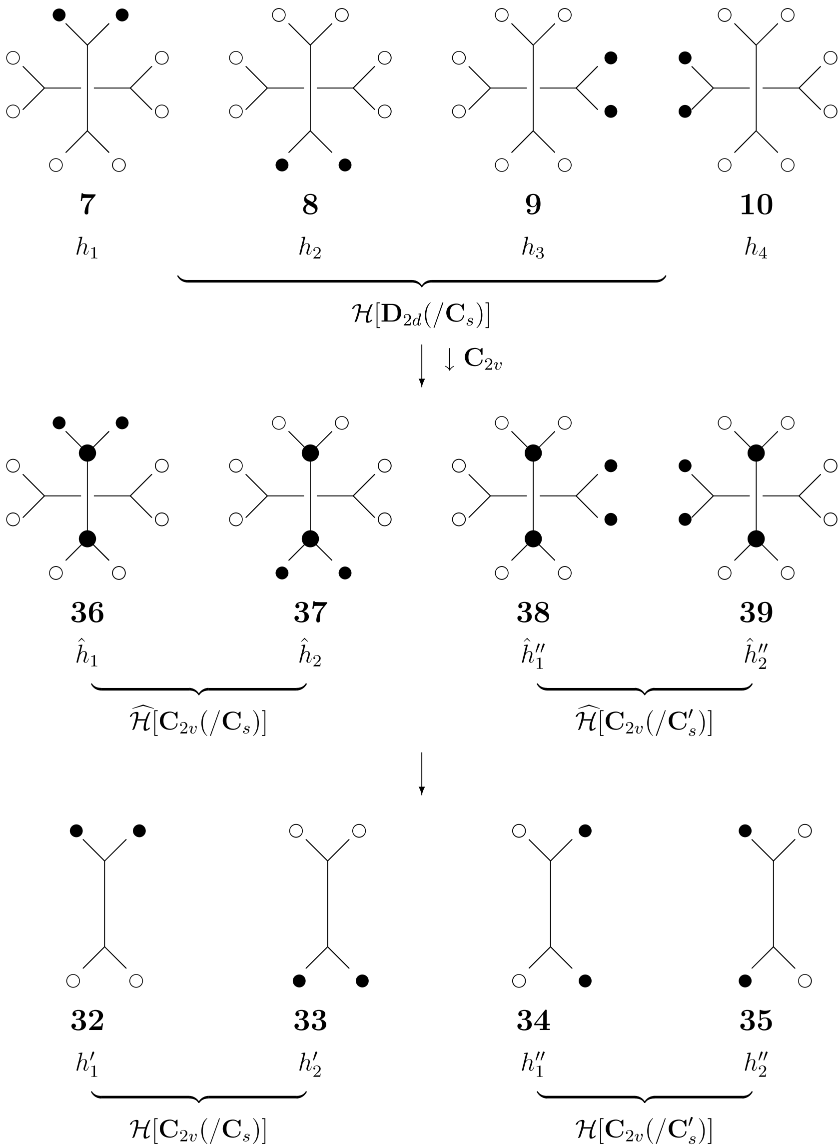

Figure 8. Double coloring for modeling a group subduction represented by $\mathbf{D}_{2d}(/\mathbf{C}_s) \downarrow \mathbf{C}_{2v} = \mathbf{C}_{2v}(/\mathbf{C}_s) + \mathbf{C}_{2v}(/\mathbf{C}'_s)$.

Then, Theorem 2 of [10] teaches us as follows:

$$\mathbf{G}(/\mathbf{G}_i) \downarrow \mathbf{G}_j = \sum_{g \in \Upsilon} \mathbf{G}_j(/g^{-1}\mathbf{G}_i g \cap \mathbf{G}_j). \tag{26}$$

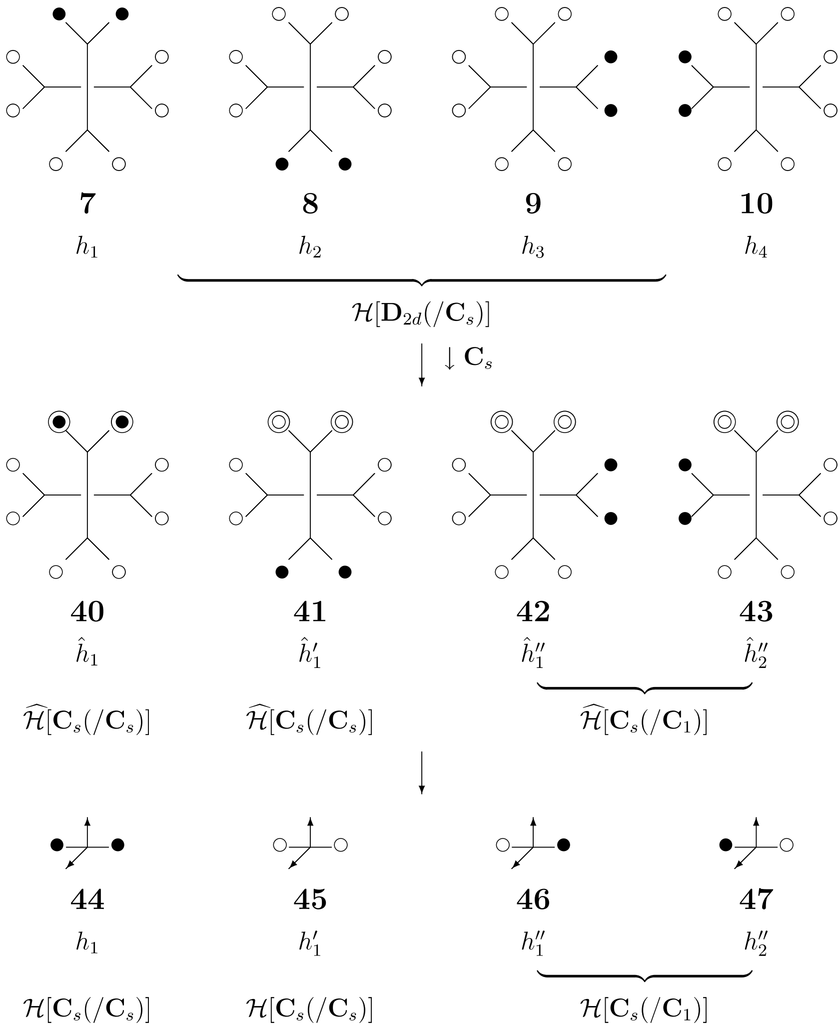

Figure 9. Double Coloring for modeling a group subduction represented by $\mathbf{D}_{2d}(/\mathbf{C}_s)\downarrow\mathbf{C}_s = 2\mathbf{C}_s(/\mathbf{C}_s) + \mathbf{C}_s(/\mathbf{C}_1)$.

Note that $g^{-1}\mathbf{G}_i g$ which is conjugate to $\mathbf{G}_i$ is the stabilizer of the coset $\mathbf{G}_i g$. The integer $|\mathbf{G}_j|/|g^{-1}\mathbf{G}_i g \cap \mathbf{G}_j|$ derived from the right-hand side of equation (26) represents the number of cosets in the double coset $\mathbf{G}_i g \mathbf{G}_j$ ($g \in \Upsilon$). This means that several cosets $\mathbf{G}_i g$ are fused under the action of $\mathbf{G}_j$ into a double coset to satisfy equation (26). This process of fusion can be modeled by the double coloring process developed in the preceding section.

From the cosets listed in equation (12), we obtain the following double coset decomposition:

$$\mathbf{D}_{2d} = \mathbf{C}_s I \mathbf{C}_{2v} + \mathbf{C}_s C_{2(1)} \mathbf{C}_{2v}, \tag{27}$$

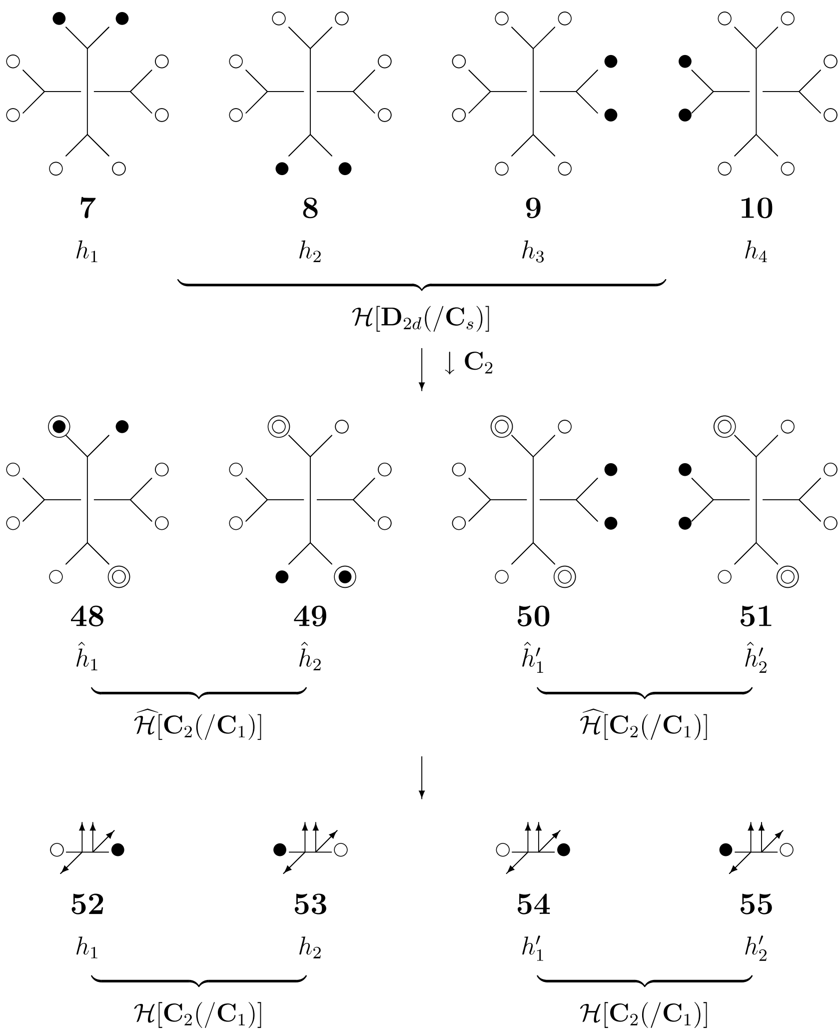

Figure 10. Double Coloring for modeling a group subduction represented by $\mathbf{D}_{2d}(/\mathbf{C}_s) \downarrow \mathbf{C}_2 = 2\mathbf{C}_2(/\mathbf{C}_1)$.

where the transversal is obtained to be $\{I, C_{2(1)}\}$. The first double coset $\mathbf{C}_s I \mathbf{C}_{2v}$ ($=\mathbf{C}_{2v}$) contains the cosets $\mathbf{C}_s$ and $\mathbf{C}_s C_{2(3)}$; and the second double coset $\mathbf{C}_s C_{2(1)} \mathbf{C}_{2v}$ contains the cosets $\mathbf{C}_s C_{2(1)}$ and $\mathbf{C}_s C_{2(2)}$.

This process is rationalized also by figure 6, which is used to model the subduction represented by $\mathbf{D}_{2d}(/\mathbf{C}_s) \downarrow \mathbf{C}_{2v} = \mathbf{C}_{2v}(/\mathbf{C}_s) + \mathbf{C}_{2v}(/\mathbf{C}'_s)$. The set of **24** and **28** (for $\mathbf{C}_s I$) and the set of **25** and **29** (for $\mathbf{C}_s C_{(3)}$) are fused under the action of $\mathbf{C}_{2v}$ so as to produce a combined set which is regarded as the first double coset of equation (27). This process correspond to $\mathbf{C}_{2v}(/\mathbf{C}_s)$, since the construction of the homomer set $\widehat{\mathcal{H}}[\mathbf{C}_{2v}(/\mathbf{C}_s)]$ equalizes the homomers (figure 6). Note

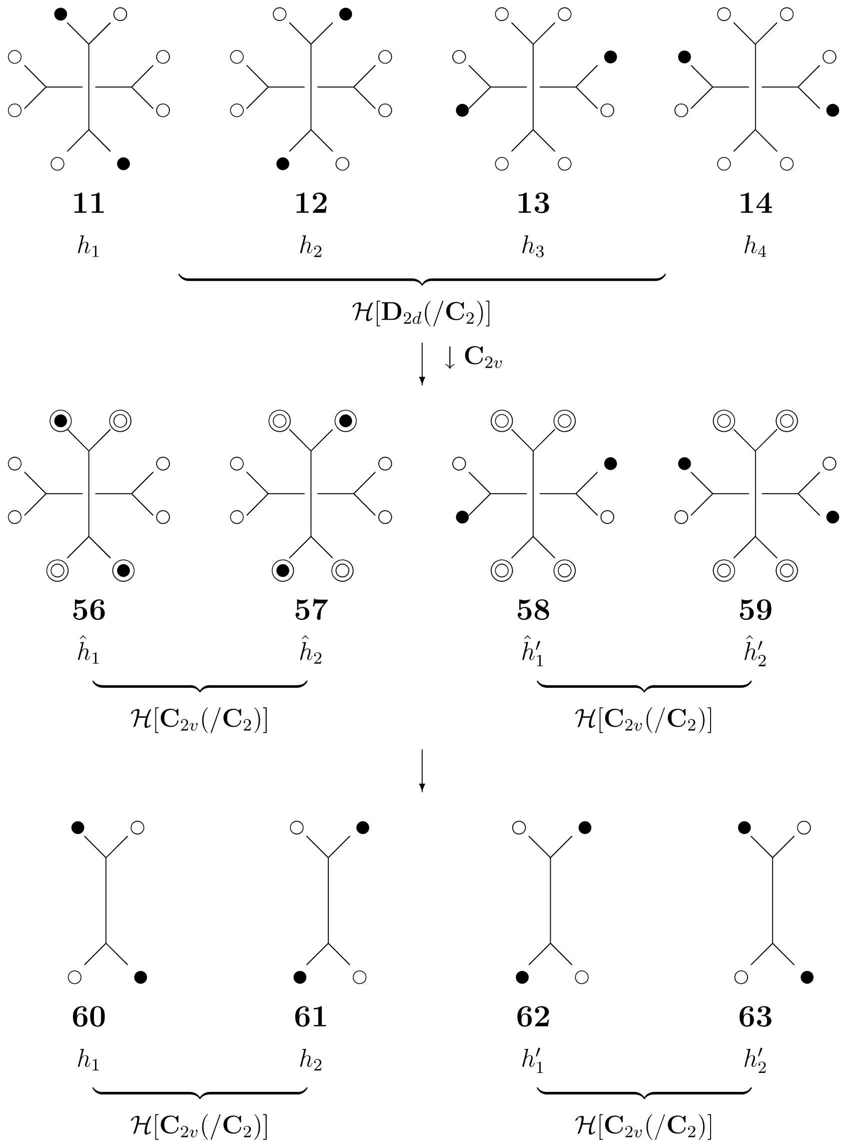

Figure 11. Direct modeling of a group subduction represented by $\mathbf{D}_{2d}(/\mathbf{C}_2) \downarrow \mathbf{C}_{2v} = 2\mathbf{C}_{2v}(/\mathbf{C}_2)$.

that $I^{-1}\mathbf{C}_s I \cap \mathbf{C}_{2v} = \mathbf{C}_s$, which appears as the local symmetry of the coset representation $\mathbf{C}_{2v}(/\mathbf{C}_s)$ in agreement with equation (26). On the other hand, the set of **26** and **30** (for $\mathbf{C}_s C_{2(1)}$) and the set of **27** and **31** (for $\mathbf{C}_s C_{(2)}$) are fused under the action of $\mathbf{C}_{2v}$, producing a combined set which is regarded as the second double coset of equation (27). This process correspond to $\mathbf{C}_{2v}(/\mathbf{C}'_s)$. Note that $C_{2(1)}^{-1}\mathbf{C}_s C_{2(1)} \cap \mathbf{C}_{2v} = \mathbf{C}'_s \cap \mathbf{C}_{2v} = \mathbf{C}'_s$, which appears as the local symmetry of the coset representation $\mathbf{C}_{2v}(/\mathbf{C}'_s)$ in agreement with equation (26). Keeping this discussion in mind, figure 7 is found to illustrate the modeling the same double coset decomposition.

Let us then consider figure 9, which models the subduction represented by $\mathbf{D}_{2d}(/\mathbf{C}_s) \downarrow \mathbf{C}_s = 2\mathbf{C}_s(/\mathbf{C}_s) + \mathbf{C}_s(/\mathbf{C}_1)$. From the cosets listed in equation (12), we obtain the following double coset decomposition:

$$\mathbf{D}_{2d} = \mathbf{C}_s I \mathbf{C}_s + \mathbf{C}_s C_{2(3)} \mathbf{C}_s + \mathbf{C}_s C_{2(1)} \mathbf{C}_s, \tag{28}$$

where the transversal is obtained to be $\{I, C_{2(3)}, C_{2(1)}\}$. The first double coset $\mathbf{C}_s I \mathbf{C}_s$ $(= \mathbf{C}_s)$ contains the coset $\mathbf{C}_s$; the second double coset $\mathbf{C}_s C_{2(3)} \mathbf{C}_s$ contains the cosets $\mathbf{C}_s C_{2(3)}$; and the third double coset $\mathbf{C}_s C_{2(1)} \mathbf{C}_s$ contains the cosets $\mathbf{C}_s C_{2(1)}$ and $\mathbf{C}_s C_{2(2)}$.

The homomer set $\widehat{\mathcal{H}}[\mathbf{C}_s(/\mathbf{C}_s)]$ (containing **40**) corresponds to the double coset $\mathbf{C}_s I \mathbf{C}_s$ appearing at equation (28). Note that $I^{-1}\mathbf{C}_s I \cap \mathbf{C}_s = \mathbf{C}_s$, which appears as the local symmetry of the coset representation $\mathbf{C}_{2v}(/\mathbf{C}_s)$ in agreement with equation (26). The homomer set $\widehat{\mathcal{H}}[\mathbf{C}_s(/\mathbf{C}_s)]$ for **41** corresponds to the double coset $\mathbf{C}_s C_{2(3)} \mathbf{C}_s$ appearing at the equation (28). Note that $C_{2(3)}^{-1}\mathbf{C}_s C_{2(3)} \cap \mathbf{C}_s = \mathbf{C}_s$, which appears as the local symmetry of the coset representation $\mathbf{C}_{2v}(/\mathbf{C}_s)$ in agreement with equation (26). The homomer set $\widehat{\mathcal{H}}[\mathbf{C}_s(/\mathbf{C}_1)]$ for **42** and **43** corresponds to the double coset $\mathbf{C}_s C_{2(1)} \mathbf{C}_s$ appearing at the equation (28). Note that $C_{2(1)}^{-1}\mathbf{C}_s C_{2(1)} \cap \mathbf{C}_s = \mathbf{C}'_s \cap \mathbf{C}_s = \mathbf{C}_1$, which appears as the local symmetry of the coset representation $\mathbf{C}_s(/\mathbf{C}_1)$ in agreement with equation (26). It follows that Fig. 9 models the double coset decomposition represented by equation (28).

6. Modeling of USCIs

The method of double coloring described above yields $\mathbf{G}(/\mathbf{G}_i) \downarrow \mathbf{G}_j$ as a sum of coset representations of the subgroup $\mathbf{G}_j$ (equation (8)). Hence, the corresponding USCIs can be easily obtained.

For example, figure 7 models $\mathbf{D}_{2d}(/\mathbf{C}_s) \downarrow \mathbf{C}_{2v} = \mathbf{C}_{2v}(/\mathbf{C}_s) + \mathbf{C}_{2v}(/\mathbf{C}'_s)$ so as to give the corresponding USCI s_2^2. Thus, figure 7 shows that the number of homomers in $\widehat{\mathcal{H}}[\mathbf{C}_{2v}(/\mathbf{C}_s)]$ is equal to 2 (also algebraically $|\mathbf{C}_{2v}|/|\mathbf{C}_s| = 4/2 = 2$) so as to give a dummy variable s_2 and that the number of homomers in $\widehat{\mathcal{H}}[\mathbf{C}_{2v}(/\mathbf{C}'_s)]$ is equal to 2 (also algebraically $|\mathbf{C}_{2v}|/|\mathbf{C}'_s| = 4/2 = 2$) so as to give a dummy variable s_2.

Figure 7 models $\mathbf{D}_{2d}(/\mathbf{C}_s) \downarrow \mathbf{C}_s = 2\mathbf{C}_s(/\mathbf{C}_s) + \mathbf{C}_s(/\mathbf{C}_1)$ so as to give the corresponding USCI $s_1^2 s_2$. Graphically, figure 7 shows that the numbers of homomers in $\widehat{\mathcal{H}}[\mathbf{C}_s(/\mathbf{C}_s)]$ and in $\widehat{\mathcal{H}}[\mathbf{C}_s(/\mathbf{C}_1)]$ are respectively equal to 1 (algebraically $|\mathbf{C}_s|/|\mathbf{C}_s| = 1$) and 2 (algebraically $|\mathbf{C}_s|/|\mathbf{C}_1| = 2$) so as to give a dummy variable s_1 and s_2. Since there are two $\widehat{\mathcal{H}}[\mathbf{C}_s(/\mathbf{C}_s)]$, we can find USCI to be $s_1^2 s_2$.

Similarly, figure 10 models $\mathbf{D}_{2d}(/\mathbf{C}_s)\downarrow\mathbf{C}_2 = 2\mathbf{C}_2(/\mathbf{C}_1)$ so as to give the corresponding USCI s_2^2 by inspection. Figure 11 models $\mathbf{D}_{2d}(/\mathbf{C}_2)\downarrow\mathbf{C}_{2v} = 2\mathbf{C}_{2v}(/\mathbf{C}_2)$ so as to give the corresponding USCI s_2^2 by inspection.

7. Conclusion

The concept of doubly-colored graphs is proposed for modeling such abstract concepts as subductions of coset representations, double cosets, and unit subduced cycle indices (USCIs). Thereby, their fruitful contents are visualized so as to be understandable graphically.

References

[1] S. Fujita, *Symmetry and Combinatorial Enumeration in Chemistry* (Springer-Verlag, Berlin, 1991).
[2] S. Fujita, Theor. Chim. Acta 76 (1989) 247–268.
[3] S. Fujita, J. Am. Chem. Soc. 112 (1990) 3390–3397.
[4] S. Fujita, Theor. Chim. Acta 78 (1990) 45–63.
[5] S. Fujita, Bull. Chem. Soc. Jpn. 64 (1991) 3313–3323.
[6] S. Fujita, J. Chem. Inf. Comput. Sci. 31 (1991) 540–546.
[7] S. Fujita and S. El-Basil, MATCH 46 (2002) 121–135.
[8] S. Fujita and S. El-Basil, J. Math. Chem. 33 (2003) 255–277.
[9] S. El-Basil, *Combinatorial Organic Chemistry; An Educational Approach* (Nova Scientific, New York, 1999).
[10] S. Fujita, J. Graph Theory 18 (1994) 349–371.